

## Supplementary Information

### Direct Z-scheme P-TiO<sub>2</sub>/g-C<sub>3</sub>N<sub>4</sub> Heterojunction for the Photocatalytic Degradation of Sulfa Antibiotics

Dai YongHeng,<sup>a</sup> Yuan Huayu,<sup>a</sup> Li Jiang,<sup>a\*</sup> Su Qj,<sup>a</sup> Yi QianWen,<sup>a</sup> Zhang YunTao,<sup>a</sup>

<sup>a</sup> College of Resources and Environmental Engineering, Guizhou University, Guiyang, Guizhou, P.R. China.

\* Correspondence at: Li Jiang (jli82@gzu.edu.cn);

\* Corresponding author: Jiang Li

E-mail: [jli82@gzu.edu.cn](mailto:jli82@gzu.edu.cn)

Address: College of Resources and Environmental Engineering, Guizhou University, Guiyang  
550025, China

## Contents

### Texts

**Text S1.** Characterization.

**Text S2.** Photocatalytic activity.

**Text S3.** Reusability and stability of photocatalyst.

**Text S4.** The quenching experiment

### Figures

**Fig.S1** Pseudo first-order rate constants of (a)SM2;(b)SMM;(c)SD;(d)SMZ.

**Fig.S2** Effect of different initial concentrations of antibiotics on photocatalytic degradation efficiency: a) SD, b) SM2, c) SMM, d) SMZ.

**Fig.S3** Effect of different concentrations of photocatalytic materials on mixed sulfonamides antibiotics: a) SD, b) SM2, c) SMM, d) SMZ.

**Fig.S4** Effect of pH of different solution on photocatalytic degradation: a) SD, b) SM2, c) SMM, d) SMZ.

**Fig.S5** Quenching experiment for the active substance.

**Fig.S6** ESR spectra of DMPO spin-trapping over CNPT-3: a)  $\text{DMPO}\cdot\text{O}^{-2}$ ; b)  $\text{DMPO}\cdot\text{OH}$ .

**Fig.S7** PL Spectra Excited of Photocatalytic Materials

**Fig. S8** (a)  $\text{g-C}_3\text{N}_4$  and (b) (c) P-TiO<sub>2</sub> photocatalytic material SEM.

**Fig.S9** Mass spectra of the Possible identified intermediates by GC–MS analyses at different illumination intervals of Sulfadiazine (a) 0 min, (b) 60 min, (c) 120 min.

**Fig.S10** Mass spectra of the Possible identified intermediates by GC–MS analyses at different illumination intervals of Sulfamethazine (a) 0 min, (b) 60 min, (c) 120 min.

**Fig.S11** Mass spectra of the Possible identified intermediates by GC–MS analyses at different illumination intervals of Sulfamonomethoxine (a) 0 min, (b) 60 min, (c) 120 min.

**Fig.S12** Mass spectra of the Possible identified intermediates by GC–MS analyses at different illumination intervals of Sulfamethoxazole (a) 0 min, (b) 60 min, (c) 120 min.

### Tables

**Table.S1** The SAs concentration in different sewage

**Table.S2** Comparison of SAs photocatalytic degradation efficiency by various photocatalysts.

## **Text S1. Characterization**

X-ray diffraction (XRD) was performed on a Bruker D8 diffractometer with Cu-K $\alpha$  ( $\lambda = 0.15406$  nm) at 45 kV and 40 mA as the radiation source. Diffraction patterns were collected in the  $2\theta$  range of  $5\sim 90^\circ$ . The morphologies of the synthesized photocatalysts samples were characterised using scanning electron microscope (SEM, JSM-6701F, JEOL, Japan) and transmission electron microscopy (TEM, JEM-2100F, Hitachi, Japan) operating at 5kV. The elemental composition of the synthesized samples was obtained by X-ray photoelectron spectroscopy (XPS) (XPS, ESCALAB 250Xi, ThermoFisher Ltd., USA). UV-vis diffuse reflectance spectra (DRS) were observed via a LAMBDA 1050 spectrophotometer (PerkinElmer, USA) from 200~800 nm. The transient photocurrent responses, Electrochemical impedance spectroscopy (EIS) spectra and Mott-Schottky plots were detected by an electrochemical workstation (CHI 760E, Shanghai Chenhua Instrument Co., China) with a standard three-electrode cell including a photocatalyst working electrode, a Pt wire counter electrode, and a standard saturated calomel electrode (SCE) as reference electrode.

## **Text S2. Photocatalytic activity**

Experiments on the degradation of antibiotic by photocatalysts were performed in a quartz sleeve photoreactor, which was placed on a magnetic stirrer at a rotation speed of 350 rpm. The experiments use the Xe lamp (YM-GHX-XE-300) to simulate the irradiation of sunlight, 20 mg of the photocatalysts were added to 50 mL of the four mixed sulfonamide antibiotics solution ( $10 \text{ mg}\cdot\text{L}^{-1}$ ) in a quartz photoreactor. The initial pH was adjusted with 1 M HCl or NaOH. After adsorption-desorption equilibrium was achieved by 30 min of stirring in darkness carry out photocatalytic degradation experiments. Moreover, approximately 3 mL of the suspensions were sampled at decided time intervals, followed by filtering with syringe membrane filters ( $0.22 \mu\text{m}$ ) to remove catalyst particulates. The concentration of antibiotics was determined by LC-MS (LC: Agilent Technologies 1290 Infinity; MS: AB SCIEXQTRAP 6470, Agilent, USA).

The degradation rate of antibiotics is shown in Eq (1):  $Y = (1 - C_t/C_0) \times 100\%$  Eq (1)

In the formula, where Y is the degradation rate of the antibiotic;  $C_0$  is initial concentration of four mixed sulfonamide antibiotics;  $C_t$  is the time dependent concentration of four mixed sulfonamide antibiotics.

## **Text S3. Reusability and stability of photocatalyst**

The solution after photocatalytic reaction was collected in the centrifugal tube, and the light yellow precipitate was obtained after centrifugation. The precipitate was dried at 80°C and then ground for use. Finally, the dried photocatalyst is added to the sulfa mixture for reuse.

#### Text S4. The quenching experiment

The active substances in the photocatalytic reaction system, including photoinduced holes ( $h^+$ ), photoinduced electrons ( $e^-$ ), hydroxyl radical ( $\cdot OH$ ) and superoxide radical ( $\cdot O_2^-$ ), may participate in the photocatalytic process. The active substances  $\cdot OH$ ,  $e^-$ ,  $\cdot O_2^-$  and  $h^+$  were quenched by isopropanol (IPA), potassium dichromate ( $K_2Cr_2O_7$ ),  $N_2$  and sodium oxalate ( $Na_2C_2O_4$ ) to explore the beneficial active substances produced in the reaction system.

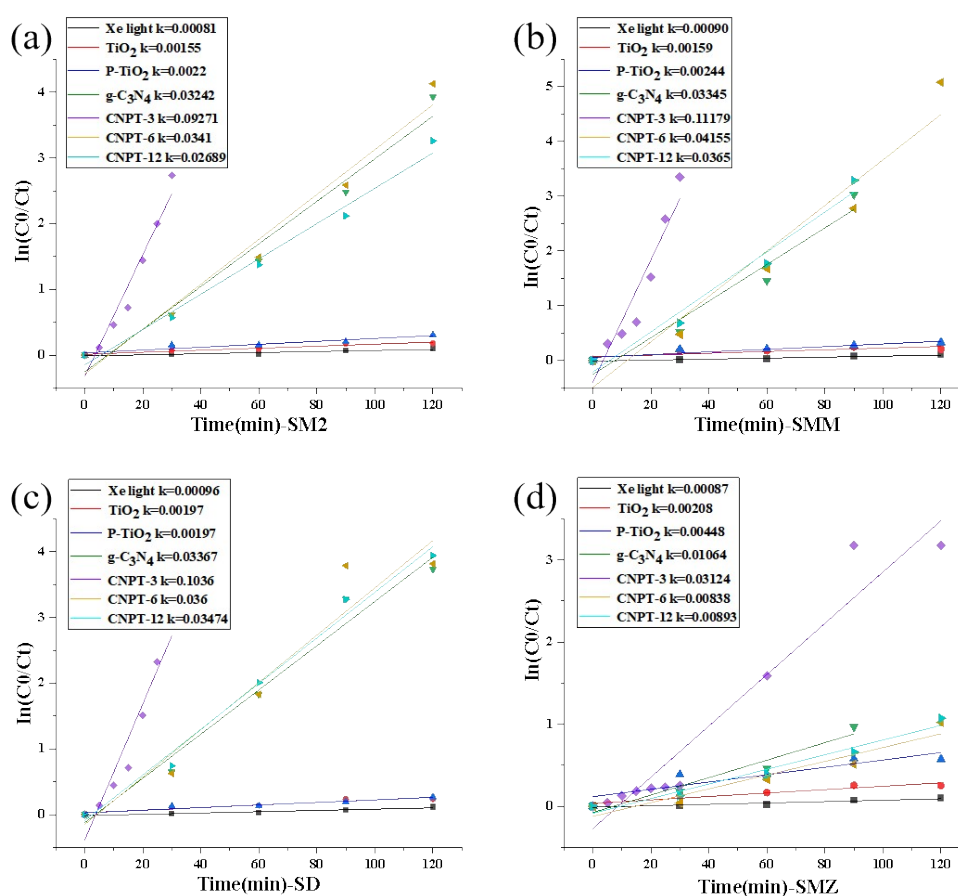


Fig.S1 Pseudo first-order rate constants of (a)SM2;(b)SMM;(c)SD;(d)SMZ.

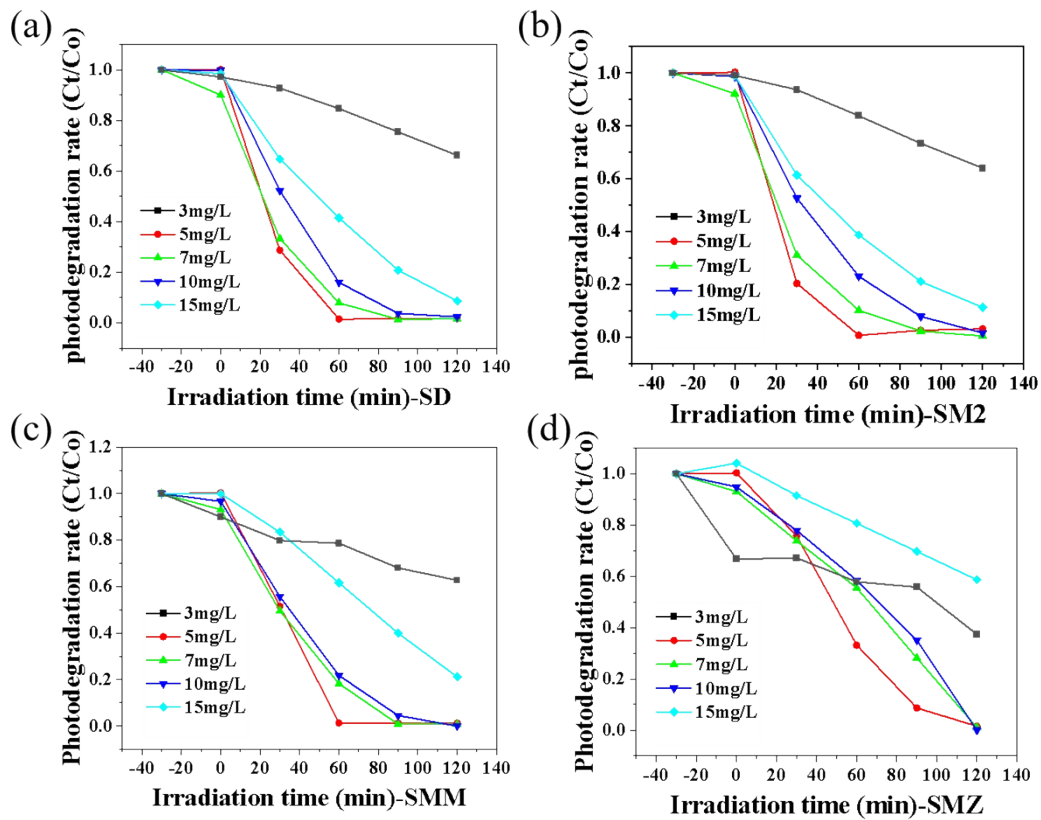


Fig.S2 Effect of different initial concentrations of antibiotics on photocatalytic degradation efficiency: a) SD, b) SM2, c) SMM, d) SMZ.

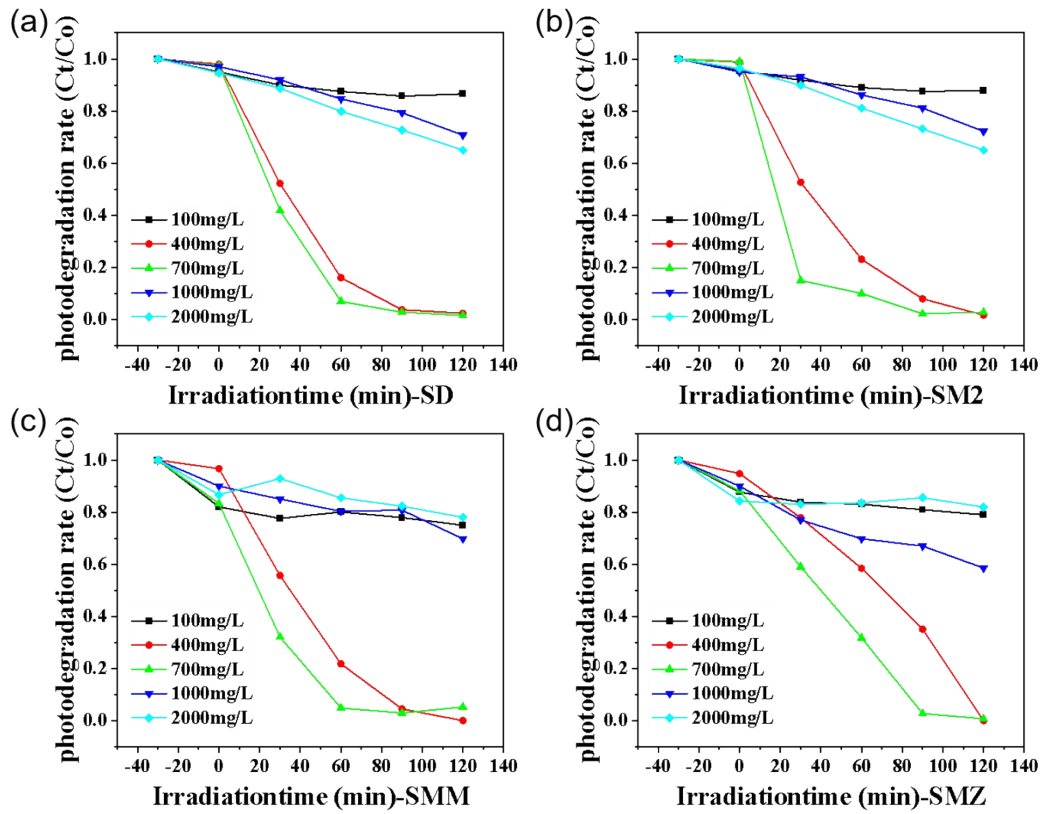


Fig.S3 Effect of different concentrations of photocatalytic materials on mixed sulfonamides antibiotics: a) SD, b) SM2, c) SMM, d) SMZ.

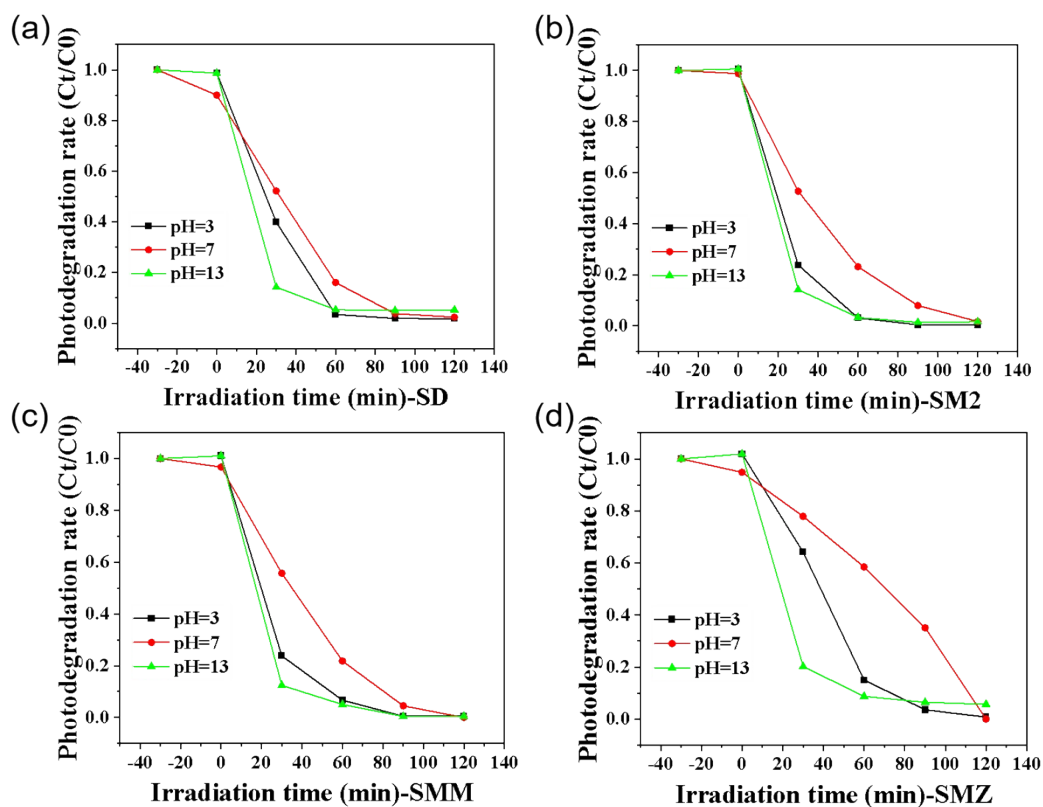


Fig.S4 Effect of pH of different solution on photocatalytic degradation: a) SD, b) SM2, c) SMM, d) SMZ.

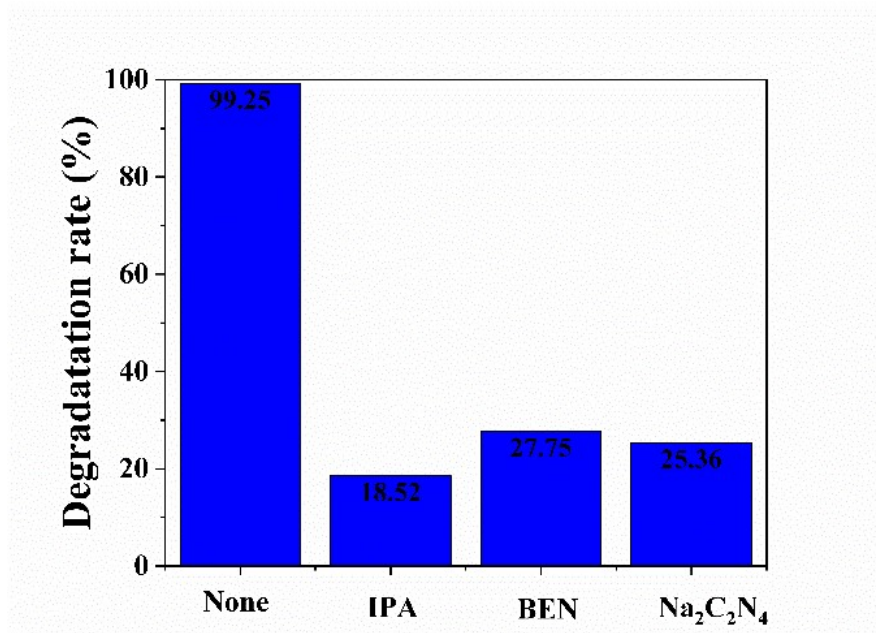


Fig. S5. Quenching experiment for the active substance.

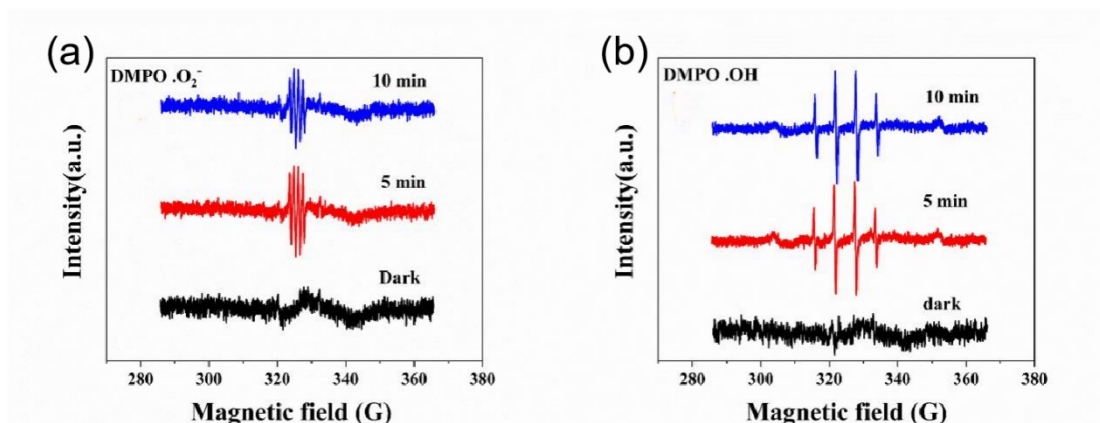


Fig.S6 ESR spectra of DMPO spin-trapping over CNPT-3: a) DMPO·O<sub>2</sub><sup>-</sup>; b) DMPO·OH.

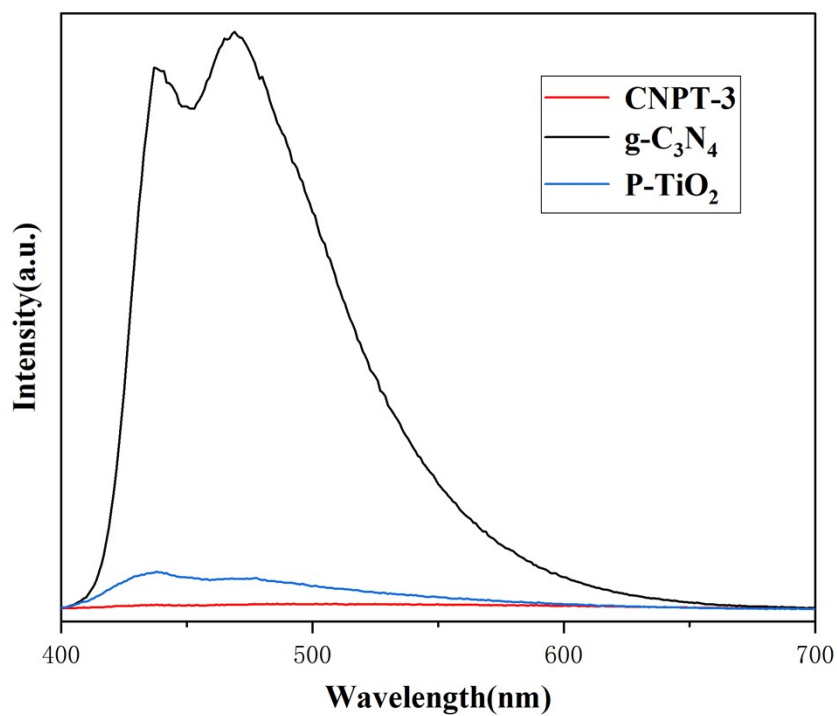


Fig.S7 PL Spectra Excited of Photocatalytic Materials



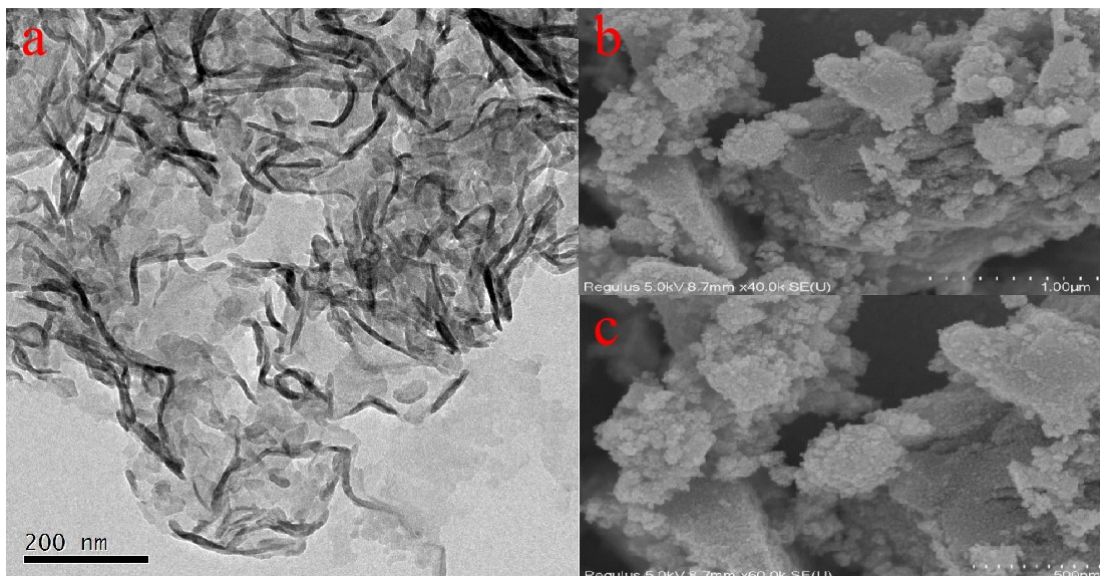
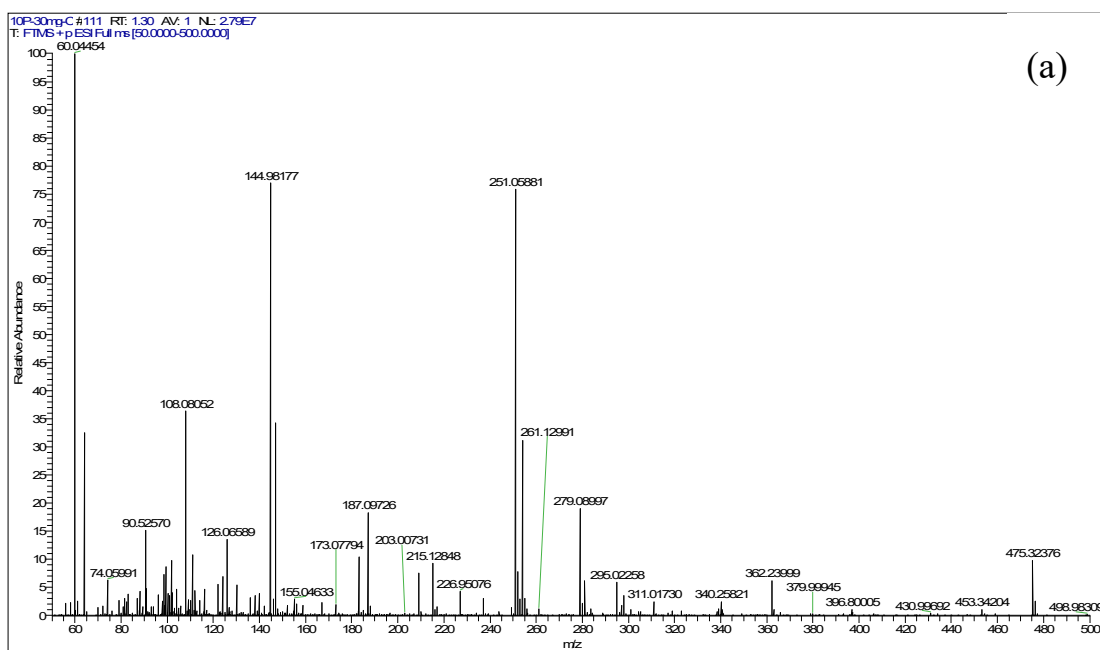


Fig. S8 (a) g-C<sub>3</sub>N<sub>4</sub> and (b) (c) P-TiO<sub>2</sub> photocatalytic material SEM.



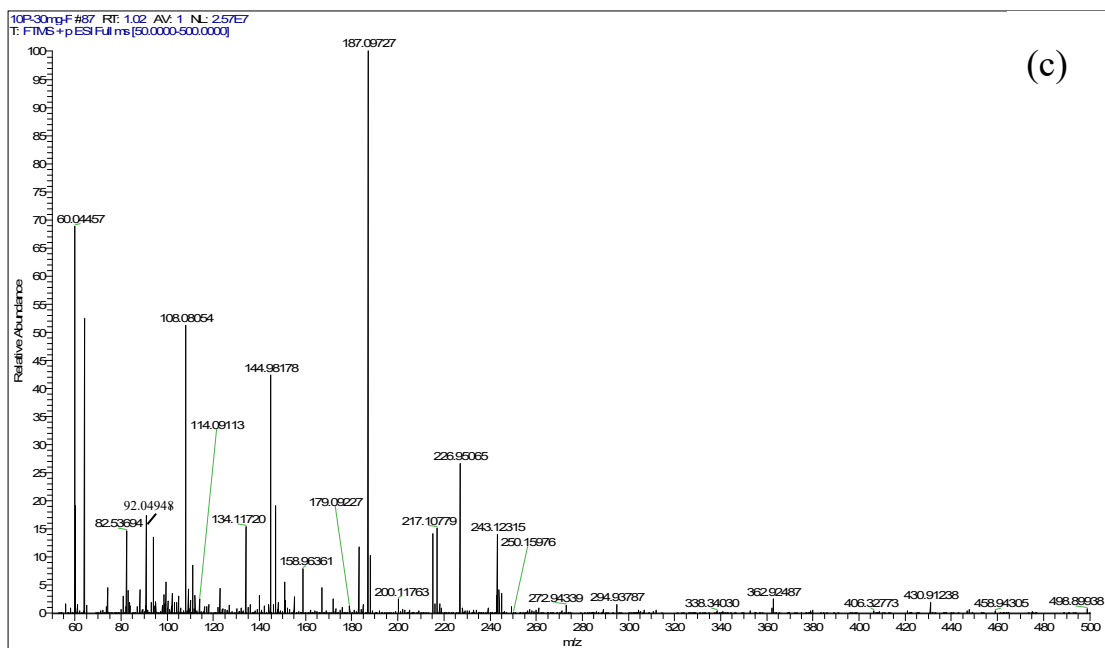
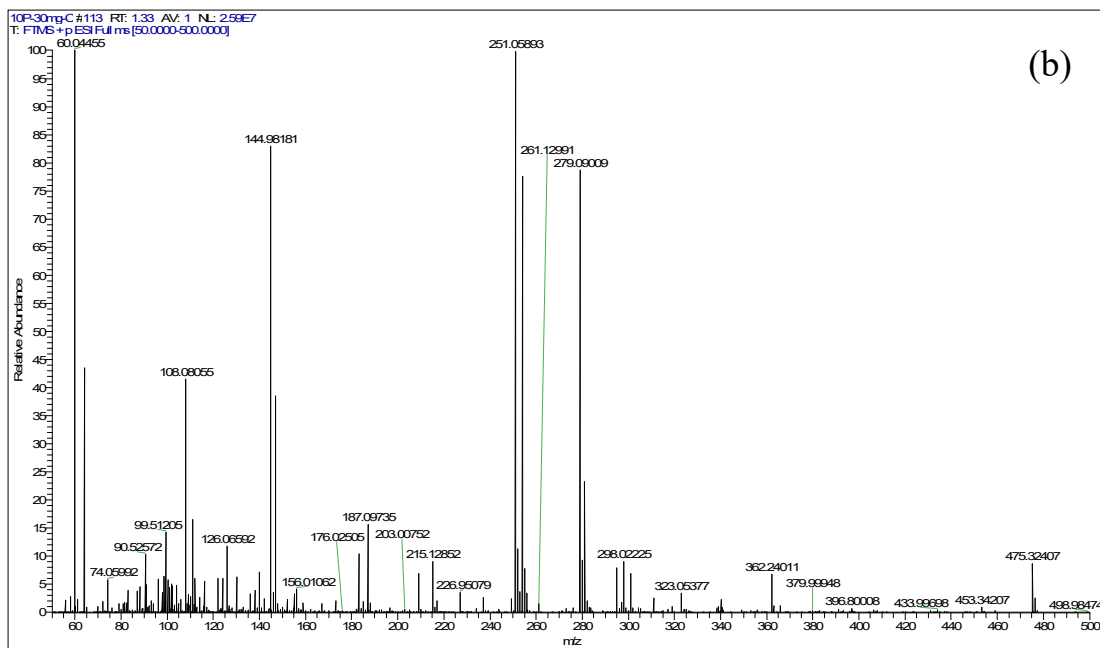
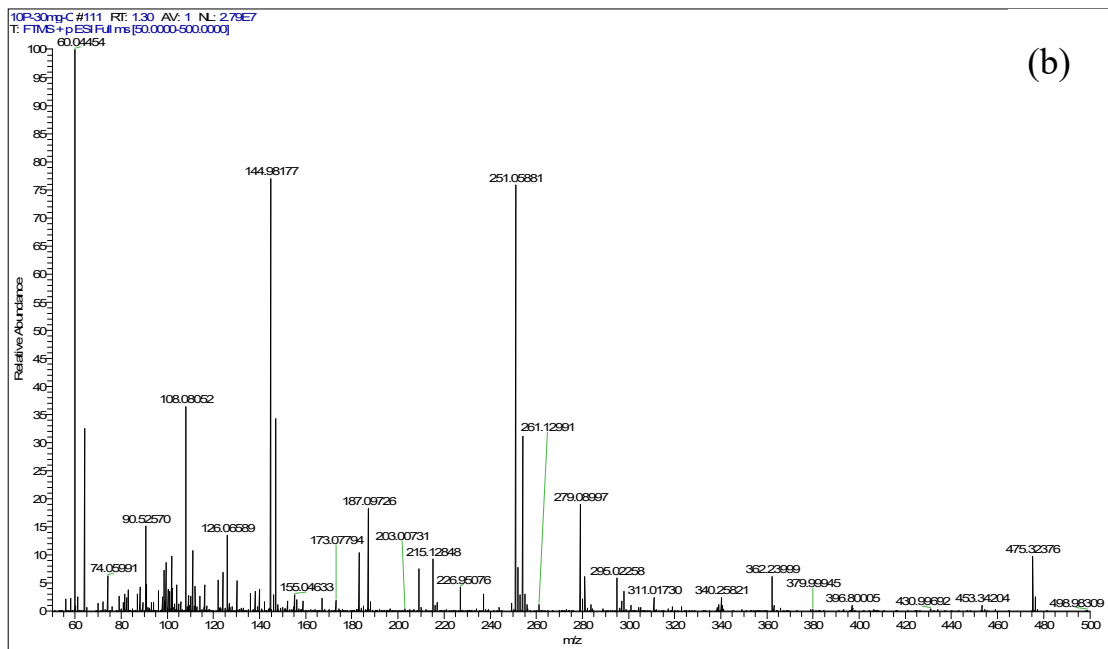
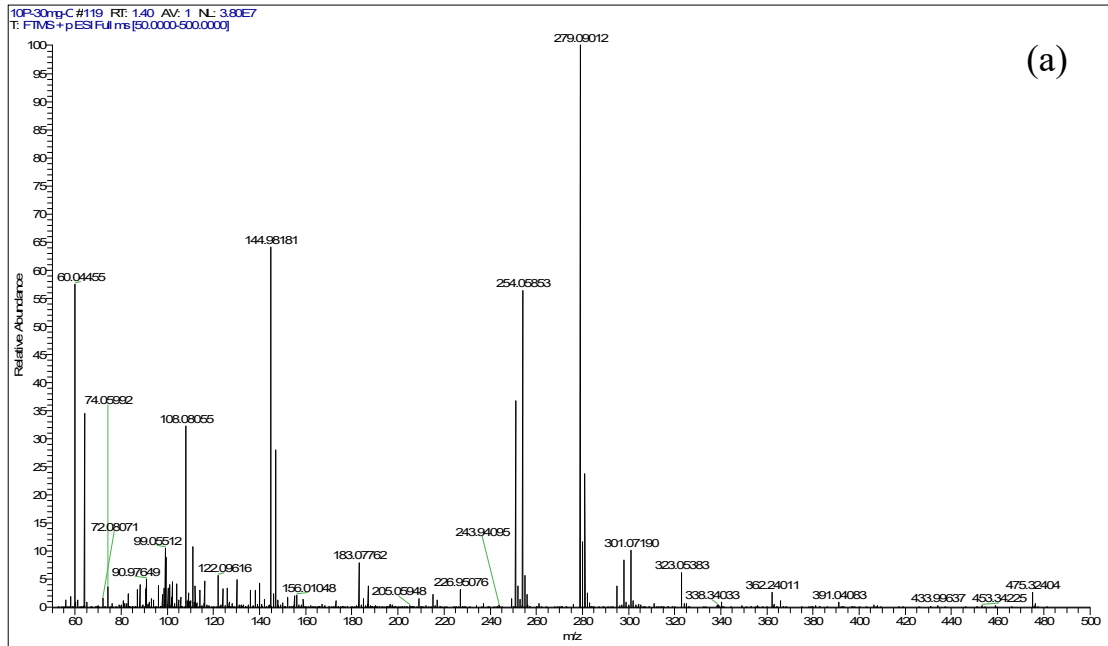


Fig. S9 Mass spectra of the Possible identified intermediates by GC-MS analyses at different illumination intervals of Sulfadiazine (a) 0 min, (b) 60 min, (c) 120 min.



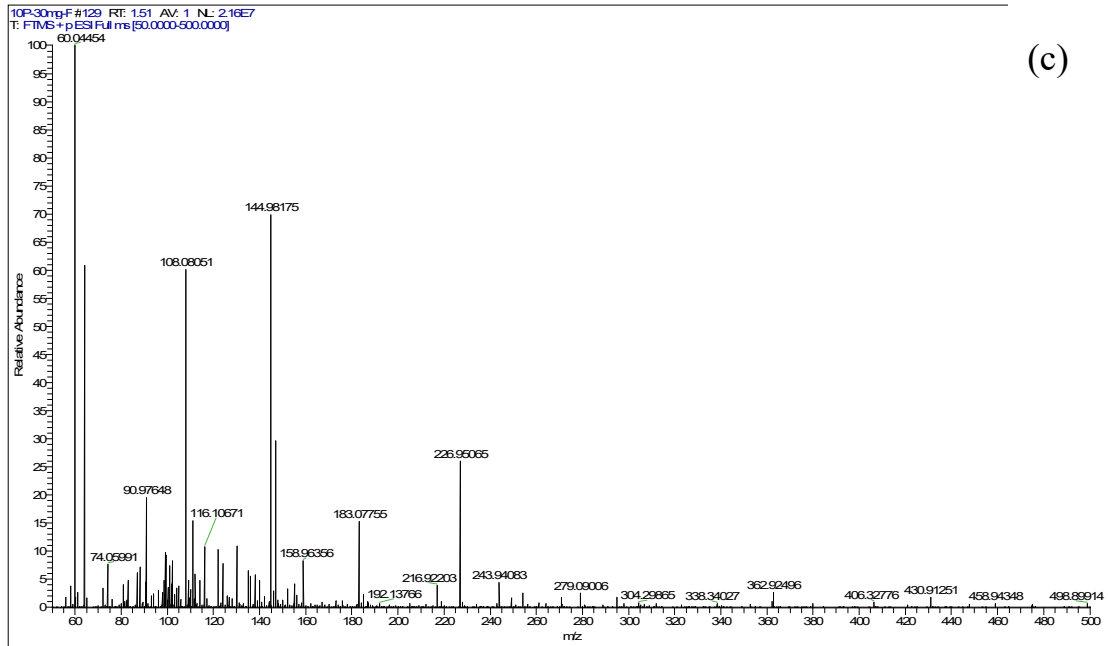
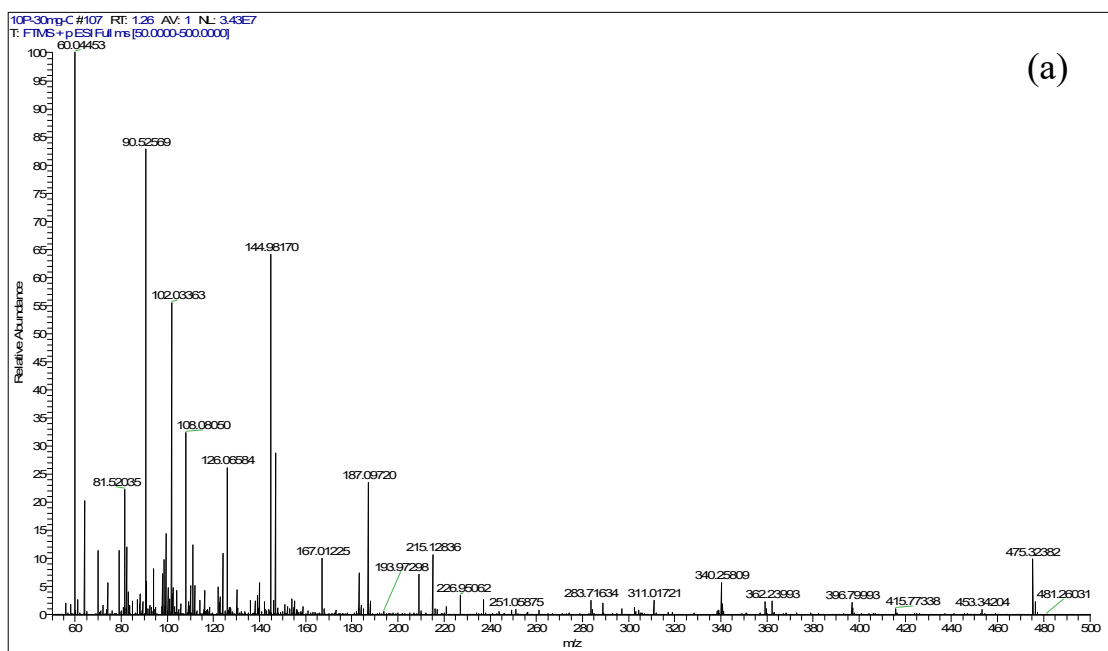


Fig. S10 Mass spectra of the Possible identified intermediates by GC-MS analyses at different illumination intervals of Sulfamethazine (a) 0 min, (b) 60 min, (c) 120 min.



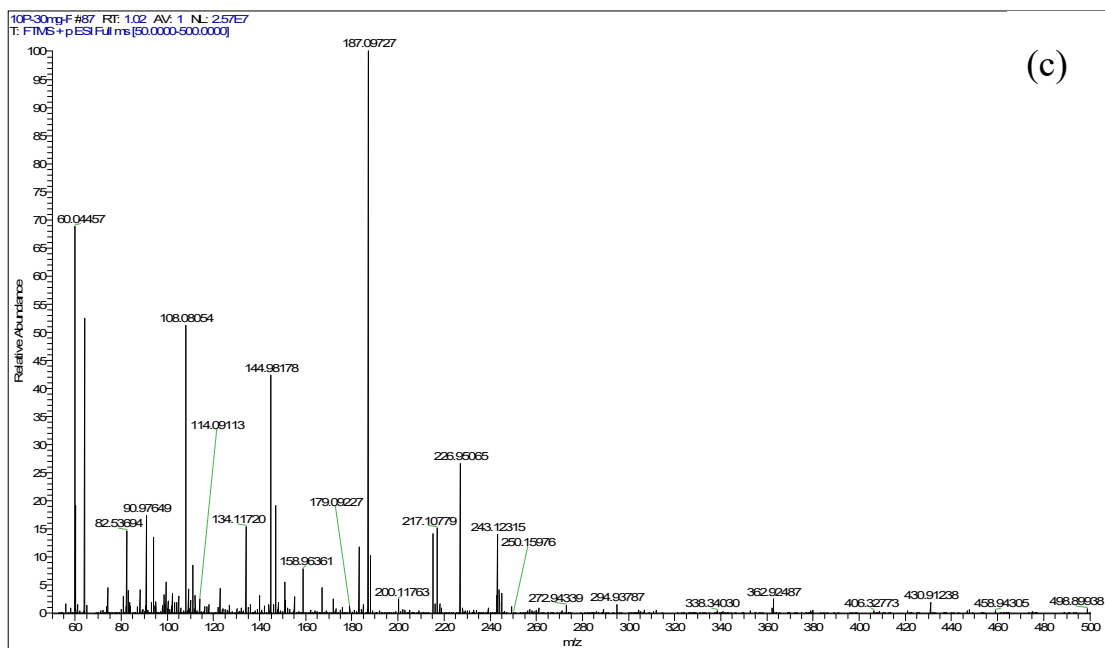
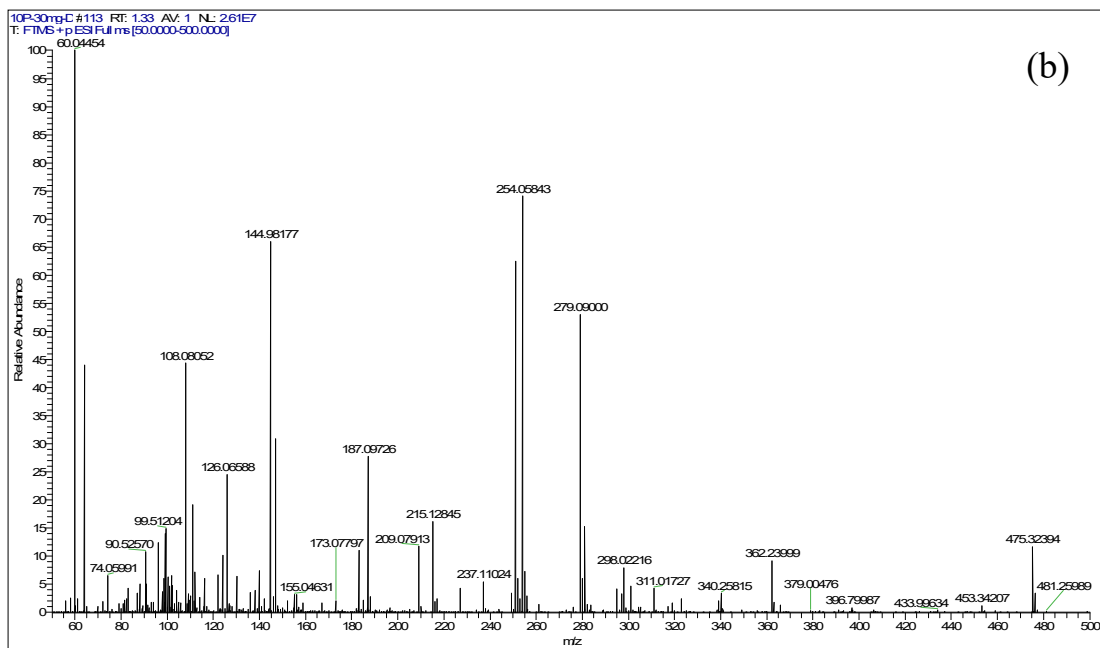
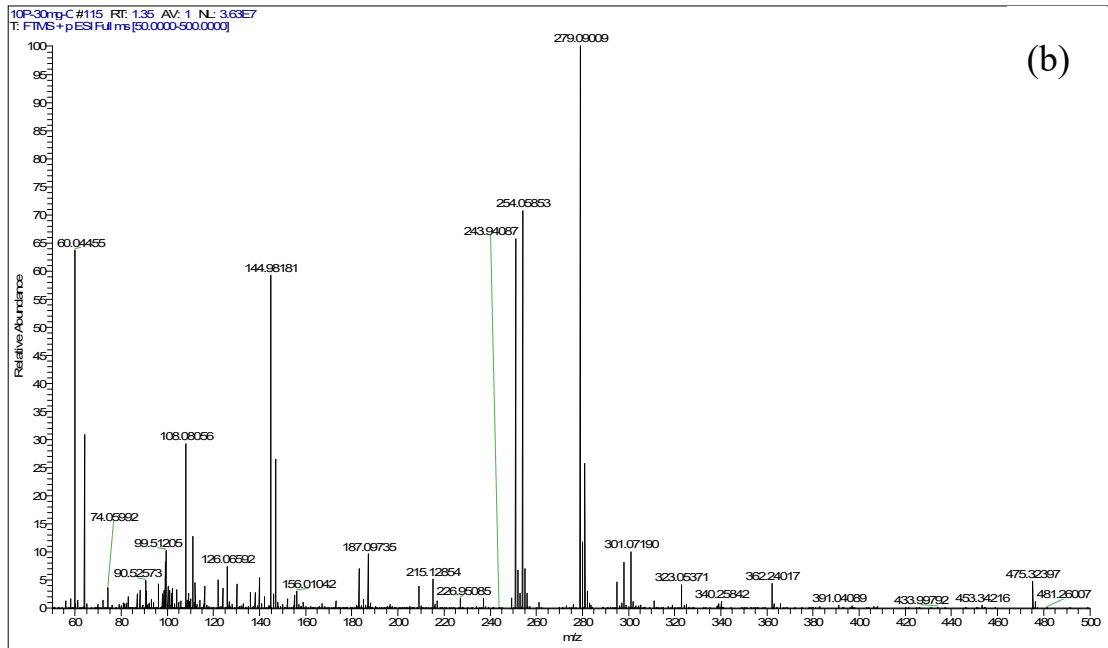
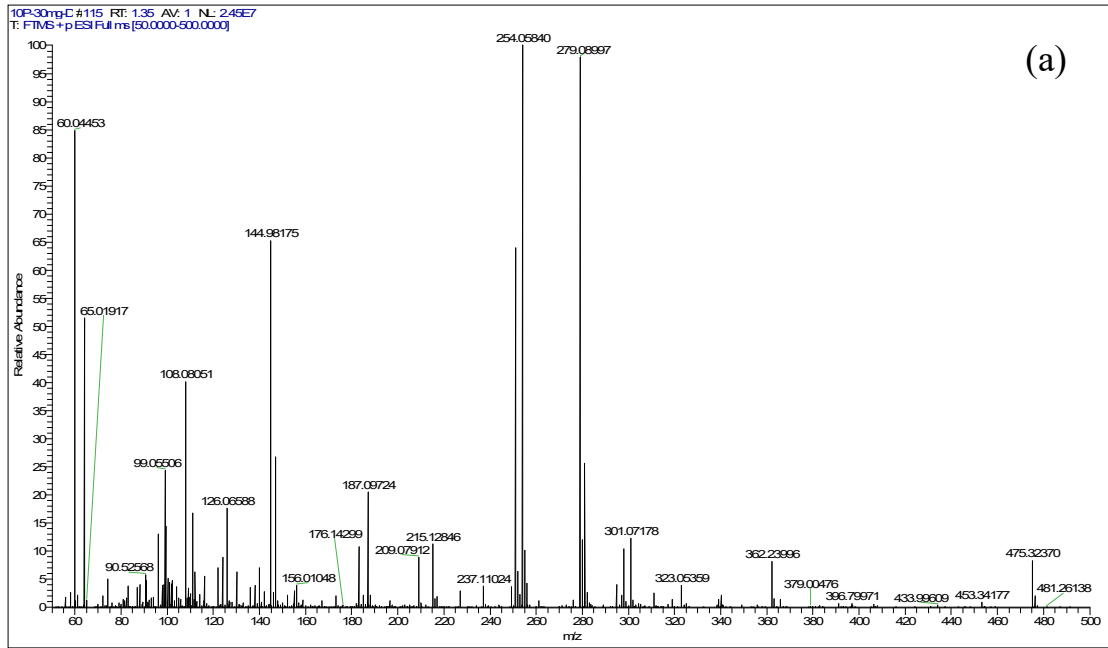


Fig. S11 Mass spectra of the Possible identified intermediates by GC-MS analyses at different illumination intervals of Sulfamonomethoxine (a) 0 min, (b) 60 min, (c) 120 min.



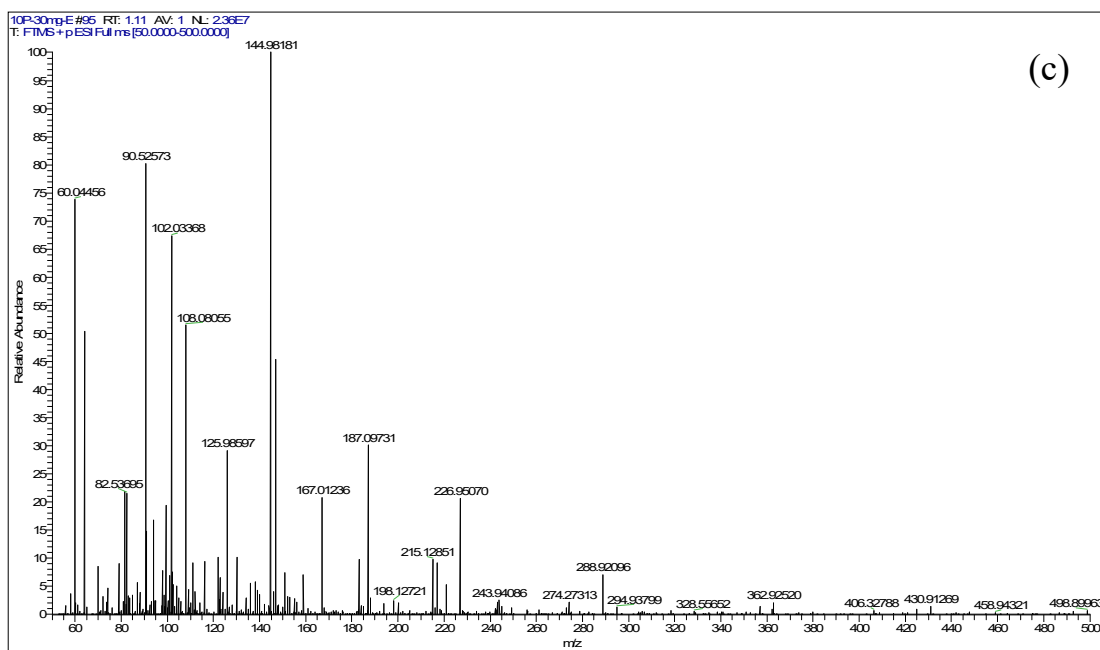


Fig. S12 Mass spectra of the Possible identified intermediates by GC–MS analyses at different illumination intervals of Sulfamethoxazole (a) 0 min, (b) 60 min, (c) 120 min.

Table.S1 The SAs concentration in different sewage

Types of antibiotics	Types of polluted water sources	Country	Concentration	Reference
Sulfamethoxazole	Effluent water	USA	18-910 ng/L	[1]
Sulfamethoxazole	Effluent water	Canada	519 ng/L	[2]
Sulfamethoxazole	Effluent water	Germany	300-1500 ng/L	[3]
Sulfamethoxazole	Surface water	USA	34-1020 ng/L	[4]
Sulfamethoxazole	Surface water	Germany	480 ng/L	[5]
Sulfamethoxazole	Surface water	China	3.68-529.4 ng/L	[6]
Sulfamethoxazole	Groundwater	USA	30-220 ng/L	[7]
Sulfamethoxazole	Groundwater	China	7.87-26.1 ng/L	[8]
Sulfadiazine	Pharmaceutical wastewater	Northern Croatia	3-20 $\mu$ g/L	[9]
Sulfamethazine	Pharmaceutical wastewater	Northern Croatia	6.7-231 $\mu$ g/L	[9]
sulfadiazine	Natural water	The Yellow River	0.017-196.16 ng/L	[10]
sulfamethoxazole	Natural water	The Yellow River	0.65-601.83 ng/L	[10]
sulfamethazine	WWTPs	Korea	1.64–1629 $\mu$ g/L	[11]
sulfamethazine	WWTPs	China	35.0–45.0 $\mu$ g/L	[11]

Table.S2 Comparison of SAs photocatalytic degradation efficiency by various photocatalysts.

Material	Dosage (g/L)	Initial concentration	Removal efficiency	References
$g-C_3N_4/ZnO$	0.65	Sulfamethoxazole 10 mg/L	96.91%, 80 min	[12]
P-TiO <sub>2</sub>	1	sulfamethazine 10 mg/L	90.5%, 300min	[13]

Biochar/ TiO <sub>2</sub>	5	Sulfamethoxazole 10 mg/L	91%, 360 min	[14]
Bisphenol S/g- C <sub>3</sub> N <sub>4</sub> /boron nitride quantum dots	0.25	Sulfadiazine 20 mg/L	100%, 60min	[15]
P-TiO <sub>2</sub> /g-C <sub>3</sub> N <sub>4</sub>	0.4	Sulfadiazine Sulfamethazine Sulfamonomethoxine Sulfamethoxazole 10 mg/L	99.3%, 120min 99.6%, 120min 99.1%, 120min 99.0%, 120min	This work

## References:

- [1] Kostich M S, Batt A L, Lazorchak J M. Concentrations of prioritized pharmaceuticals in effluents from 50 large wastewater treatment plants in the US and implications for risk estimation[J]. *Environmental pollution*, 2014, 184: 354-359. <https://doi.org/10.1016/j.envpol.2013.09.013>
- [2] Basiuk M, Brown R A, Cartwright D, et al. Trace organic compounds in rivers, streams, and wastewater in southeastern Alberta, Canada[J]. *Inland Waters*, 2017, 7(3): 283-296. <https://doi.org/10.1080/20442041.2017.1329908>
- [3] Hartig C, Storm T, Jekel M. Detection and identification of sulphonamide drugs in municipal waste water by liquid chromatography coupled with electrospray ionisation tandem mass spectrometry[J]. *Journal of Chromatography A*, 1999, 854(1-2): 163-173. [https://doi.org/10.1016/S0021-9673\(99\)00378-7](https://doi.org/10.1016/S0021-9673(99)00378-7)
- [4] Lindsey M E, Meyer M, Thurman E M. Analysis of trace levels of sulfonamide and tetracycline antimicrobials in groundwater and surface water using solid-phase extraction and liquid



chromatography/mass spectrometry[J]. *Analytical chemistry*, 2001, 73(19): 4640-4646.

<https://doi.org/10.1021/ac010514w>

[5] Hirsch R, Ternes T A, Haberer K, et al. Determination of antibiotics in different water compartments via liquid chromatography–electrospray tandem mass spectrometry[J]. *Journal of chromatography A*, 1998, 815(2): 213-223. [https://doi.org/10.1016/S0021-9673\(98\)00335-5](https://doi.org/10.1016/S0021-9673(98)00335-5)

[6] Jiang Y, Li M, Guo C, et al. Distribution and ecological risk of antibiotics in a typical effluent–receiving river (Wangyang River) in north China[J]. *Chemosphere*, 2014, 112: 267-274. <https://doi.org/10.1016/j.chemosphere.2014.04.075>

[7] Stackelberg P E, Gibs J, Furlong E T, et al. Efficiency of conventional drinking-water-treatment processes in removal of pharmaceuticals and other organic compounds[J]. *Science of the Total Environment*, 2007, 377(2-3): 255-272. <https://doi.org/10.1016/j.scitotenv.2007.01.095>

[8] Yang Y Y, Zhao J L, Liu Y S, et al. Pharmaceuticals and personal care products (PPCPs) and artificial sweeteners (ASs) in surface and ground waters and their application as indication of wastewater contamination[J]. *Science of the Total Environment*, 2018, 616: 816-823. <https://doi.org/10.1016/j.scitotenv.2017.10.241>

[9] Bielen A, Šimatović A, Kosić-Vukšić J, et al. Negative environmental impacts of antibiotic-contaminated effluents from pharmaceutical industries[J]. *Water research*, 2017, 126: 79-87. <https://doi.org/10.1016/j.watres.2017.09.019>

[10] Wang L, Wang Y, Li H, et al. Occurrence, source apportionment and source-specific risk assessment of antibiotics in a typical tributary of the Yellow River basin[J]. *Journal of Environmental Management*, 2022, 305: 114382. <https://doi.org/10.1016/j.jenvman.2021.114382>

[11] Kim J P, Jin D R, Lee W, et al. Occurrence and removal of veterinary antibiotics in livestock

wastewater treatment plants, South Korea[J]. Processes, 2020, 8(6): 720.

<https://doi.org/10.3390/pr8060720>

[12] Sun Q, Sun Y, Zhou M, et al. A 2D/3D g-C<sub>3</sub>N<sub>4</sub>/ZnO heterojunction enhanced visible-light driven photocatalytic activity for sulfonamides degradation[J]. Ceramics International, 2022, 48(5): 7283-7290. <https://doi.org/10.1016/j.ceramint.2021.11.289>

[13] Mendiola-Alvarez S Y, Hernández-Ramírez M A, Guzmán-Mar J L, et al. Phosphorous-doped TiO<sub>2</sub> nanoparticles: synthesis, characterization, and visible photocatalytic evaluation on sulfamethazine degradation[J]. Environmental Science and Pollution Research, 2019, 26(5): 4180-4191. <https://doi.org/10.1007/s11356-018-2314-6>

[14] Kim J R, Kan E. Heterogeneous photocatalytic degradation of sulfamethoxazole in water using a biochar-supported TiO<sub>2</sub> photocatalyst[J]. Journal of environmental management, 2016, 180: 94-101. <https://doi.org/10.1016/j.jenvman.2016.05.016>

[15] Zhang Q, Peng Y, Lin Y, et al. Bisphenol S-doped g-C<sub>3</sub>N<sub>4</sub> nanosheets modified by boron nitride quantum dots as efficient visible-light-driven photocatalysts for degradation of sulfamethazine[J]. Chemical Engineering Journal, 2021, 405: 126661. <https://doi.org/10.1016/j.cej.2020.126661>